

# Evaluation of the toxicity of ZnO nanoparticles to *Chlorella vulgaris* by use of the chiral perturbation approach

Hui Zhou · Xiaojun Wang · Ying Zhou · Hongzhou Yao ·  
Farooq Ahmad

Received: 30 September 2013 / Revised: 13 March 2014 / Accepted: 17 March 2014 / Published online: 22 April 2014  
© Springer-Verlag Berlin Heidelberg 2014

**Abstract** The toxicity of ZnO nanoparticles (NPs) has been widely investigated because of their extensive use in consumer products. The mechanism of the toxicity of ZnO NPs to algae is unclear, however, and it is difficult to differentiate between particle-induced toxicity and the effect of dissolved  $Zn^{2+}$ . In the work discussed in this paper we investigated particle-induced toxicity and the effects of dissolved  $Zn^{2+}$  by using the chiral perturbation approach with dichlorprop (DCPP) as chiral perturbation factor. The results indicated that intracellular zinc is important in the toxicity of ZnO NPs, and that ZnO NPs cause oxidative damage. According to dose–response curves for DCPP and the combination of ZnO NPs with (*R*)-DCPP or (*S*)-DCPP, the toxicity of DCPP was too low to perturb the toxicity of ZnO NPs, so DCPP was suitable for use as chiral perturbation factor. The different glutathione (GSH) content of algal cells exposed to (*R*)-DCPP or (*S*)-DCPP correlated well with different production of reactive oxygen species (ROS) after exposure to the two enantiomers. Treatment of algae with ZnO NPs and (*R*)-DCPP resulted in reduced levels of GSH and the glutathione/oxidized glutathione (GSH/GSSG) ratio in the cells compared with the control. Treatment of algae with ZnO NPs and (*S*)-DCPP, however, resulted in no significant changes in GSH and

GSH/GSSG. Moreover, trends of variation of GSH and GSH/GSSG were different when algae were treated with  $ZnSO_4 \cdot 7H_2O$  and the two enantiomers. Overall, the chiral perturbation approach revealed that NPs aggravated generation of ROS and that released  $Zn^{2+}$  and NPs both contribute to the toxicity of ZnO NPs.

**Keywords** ZnO nanoparticles · nanotoxicity · Chiral perturbation · Reactive oxygen species ·  $Zn^{2+}$  · Algae

## Introduction

Zinc oxide nanoparticles (ZnO NPs) are important nanomaterials (NMs) that have been extensively used in industrial and consumer products, resulting in the increasing presence of NMs in the environment [1]. For example, it is estimated that 1,000 tons of skincare products containing ZnO NPs are produced annually for the global market [2]. Italian researchers have calculated that at least 25 % of the amount of sunscreen applied to the skin is washed off during bathing and swimming [3]. This implies that approximately 250 tons of these nanomaterials are potentially discharged into the water environment [4]. Compared with normal materials, the risks to health and the environment of the novel properties of NPs are unknown. The toxicity of ZnO NPs in aquatic ecosystems has, therefore, aroused much concern.

ZnO NPs have been shown to be toxic to algae [5–8], crustaceans [9, 10], bacteria [11], and fish [12, 13]. Studies of the biotoxicity of ZnO NPs suggest several mechanisms of action. Overproduction of reactive oxygen species (ROS) is believed to be a major mechanism of the toxicity of NPs [14]. Because of the large specific surface area of NPs, which endows them with high reactivity and electron density, they can interact with biomolecules [15]. During this process, chemical reactions occur and result in increased formation of

Published in the topical collection *Euroanalysis XVII* (The European Conference on Analytical Chemistry) with guest editor Ewa Bulska.

**Electronic supplementary material** The online version of this article (doi:10.1007/s00216-014-7773-0) contains supplementary material, which is available to authorized users.

H. Zhou · X. Wang · Y. Zhou · H. Yao · F. Ahmad  
College of Chemical Engineering and Materials Science, Zhejiang  
University of Technology, Hangzhou, China

Y. Zhou (✉)  
Research Center of Analysis and Measurement, Zhejiang University  
of Technology, 18 Chaowang Road, Hangzhou 310032, Zhejiang  
Province, China  
e-mail: yingzhou@zjut.edu.cn

the superoxide radical ( $O_2^-$ ), which leads to ROS accumulation and oxidative stress [16]. It has been reported that ZnO NPs disturb the balance between oxidation and anti-oxidation processes and cause oxygen stress responses in different organs of fish [13]. This mechanism of toxicity has been mainly observed in fish and cells. However the mechanism of toxicity to algae has been mostly attributed to particle dissolution [17]. The effect of particle dissolution in the mechanism of toxicity of ZnO NPs has been demonstrated in many studies. Franklin et al. [5] conducted toxicity experiments using the freshwater alga *Pseudokirchneriella subcapitata* and revealed the toxicity of ZnO nanoparticles, bulk ZnO, and  $ZnCl_2$  was comparable; with the 72-h  $IC_{50}$  value of approximately  $60 \mu g Zn L^{-1}$ ; the toxicity of ZnO NPs was attributed solely to dissolved zinc. Because dissolution of nano-ZnO can be affected by water chemistry, for example ionic components, pH, and dissolved organic matter, the effects of water chemistry on the toxicity of ZnO NPs have been investigated by several researchers [11, 18, 19]. Whether the properties of NPs are responsible for the toxicity of nano-ZnO has rarely been reported. Nano-ZnO not only has physicochemical properties associated with NPs but can also release free zinc ions which can synergistically enhance the production of ROS and cause oxidative damage in cells. Because it is challenging to distinguish between these two types of effect of nano-ZnO on algae, the exact mechanism is not clear.

Microalgae, the primary producers in the food chain, are more sensitive to contaminants than are fish and invertebrates; they are, therefore, important organisms for monitoring water quality and aquatic toxicity. Investigating the toxicity of ZnO NPs to algae and explaining the mechanism clearly is, therefore, of great importance and can potentially lead to strategies to remediate the potentially adverse effects of engineered NMs on the environment [20].

Glutathione (GSH), the most prevalent non-protein thiol in cells, is one of the most effective radical scavengers, because of its reaction with superoxide, singlet oxygen, and hydroxyl radicals to form oxidized glutathione (GSSG) [21]. GSSG is then reduced to GSH by glutathione reductase (GR). In addition, GSH has affinity for heavy metals through its sulfhydryl group or by forming phytochelatins. The glutathione redox cycle is therefore important in the toxicity caused by both oxidative stress and exposure to heavy metals. The glutathione redox cycle is a dynamic system and amounts of GSH and GSSG are affected by such chemical contaminants as chiral pesticides [22, 23]. Enantiomers of chiral pesticides may behave differently in the environment when undergoing identical physical and chemical processes and reactions [24]. Dichlorprop (DCPP) is a widely used chiral herbicide with low toxicity which does not significantly perturb Cu(II) toxicity [23]. Inducing the production of ROS has been reported to be a mechanism of its toxicity, and only the (*R*)-form is an active herbicide [25]. The responses of glutathione

system should therefore be enantioselective after DCPP treatment. Therefore, we assumed chiral perturbation was small enough not to induce an enantioselective shift in the glutathione system when dissolved zinc combined mainly with GSH, and the enantioselective shift in the glutathione system can be observed by chiral perturbation if induced generation of ROS is the cause of the toxicity of nano-ZnO.

In the work discussed in this paper a new chiral perturbation method was used, for the first time, to investigate the toxicity of nano-ZnO. The chiral herbicide dichlorprop was used as chiral perturbation factor and *Chlorella vulgaris* as test organism for evaluating the toxic mechanism of nano-ZnO. The objective was to evaluate the contributions of the properties of ZnO NPs and released Zn ion to the toxicity to algae.

## Experimental

### Chemicals and materials

ZnO NPs were purchased from Beijing Nachen S&T. Particle size and purity were determined by transmission electron microscopy (TEM; Tecnai G2 F30; Philips-FEI, Holland) and inductively coupled plasma mass spectrometry (ICP-MS; Elan DRC-e; Perkin Elmer, USA) respectively. The characteristics of the ZnO NPs are given in the Electronic Supplementary Material (Table S1, Fig. S1). Stock suspension of ZnO NPs was prepared in algal culture medium BG11 and sonicated for 30 min before use.  $Zn^{2+}$  stock solution ( $200 mg L^{-1}$ ) was prepared by dissolving zinc sulfate heptahydrate ( $ZnSO_4 \cdot 7H_2O$ ) in the same medium. (*R*)-DCPP and (*S*)-DCPP of 99 % purity were kindly provided by the Liu W. P. research group at Zhejiang University, China. All other reagents were analytical grade. All glassware was acid washed in 10 % concentrated  $HNO_3$ , thoroughly rinsed with Milli-Q water, and sterilized before use.

### Algae bioassays

The unicellular green algae (*Chlorella vulgaris*) used in this study were obtained from the Institute of Wuhan Hydrobiology, Chinese Academy of Sciences. The algal cells were cultured in the BG11 medium at  $23 \pm 1$  °C in an incubator under illumination at 4500 lux with daily cycles of 12-h light and 12-h dark. The algal cells, in logarithmic growth phase, were cultured in 100 mL culture medium in the presence or absence of the test materials in 250-mL Erlenmeyer flasks. The initial cell density was  $1 \times 10^6$  cells  $mL^{-1}$ . During incubation, the cultures were shaken five times per day to ensure optimum growth. *Chlorella vulgaris* were exposed to a series of concentrations of nano-ZnO and  $Zn^{2+}$  (1, 5, 10, 20, 50, and 100  $\mu mol L^{-1}$ ), and (*R*)-DCPP and (*S*)-DCPP (20, 50, 100, 200, and 400  $\mu mol L^{-1}$ ). To investigate the effect of the chiral

herbicide DCPD on ZnO NPs, the two enantiomers of DCPD (50  $\mu\text{mol L}^{-1}$ ) with three concentrations of ZnO NPs or  $\text{Zn}^{2+}$  (5, 10, or 20  $\mu\text{mol L}^{-1}$ ) were added to the medium for 72 h, and inhibition of algal growth was monitored as an index to evaluate the toxicity of the materials. Three replicates were performed for each concentration. Cell density was monitored spectrophotometrically at 684 nm every 24 h by use of a spectrophotometer (UNICO 2802S) combined with a hemocytometer. The regression equation for the relationship between cell density ( $y \times 10^6$  cells  $\text{mL}^{-1}$ ) and absorption at 684 nm ( $x$ ) was calculated as  $y = 25.45x - 0.737$  ( $p < 0.01$ ,  $R = 0.996$ ).

#### ICP–MS detection of elemental Zn concentration

ICP–MS was used to quantify zinc ion released from ZnO NPs upon their interaction with the algae. The cell-wall-bound and intracellular  $\text{Zn}^{2+}$  content were determined by use of the procedure of Wang et al. [26]. After incubation for 72 h, treated algae were collected to analyze zinc concentration. Before quantification, the treated algae were centrifuged (4,000 rpm, 15 min). The algal pellets were rinsed with PBS to remove unbound zinc, then rinsed with EDTA to complex Zn bound to cell walls, and finally centrifuged. The collected supernatant was measured as cell-wall-bound zinc. The algal pellets were acid-digested and analyzed for intracellular zinc by use of ICP–MS.

#### Assessment of oxidative damage

The concentration of malondialdehyde (MDA), a molecular indicator of lipid peroxidation, was determined by use of the thiobarbituric acid (TBA) reaction. Superoxide dismutase (SOD) activity, which reflects the ability of organisms to remove superoxide radicals, was assayed by use of the xanthine–xanthine oxidase and hydroxylamine system. Commercial kits for measurement of all biochemical data were purchased from Nanjing Jiancheng Bioengineering Institute (Nanjing, China).

#### Determination of GSH and GSSG

Algae were incubated with different concentrations of the test materials for 72 h. After centrifugation, the algal pellets were frozen and thawed five times then centrifuged at 10,000 rpm for 5 min at 4 °C. The supernatant was collected for use. GSSG content was measured by use of the 5,5'-dithiobis(2-nitrobenzoic acid) (DTNB) and GSH (GSSG) recycling system. The amount of GSH was calculated by subtracting the amount of GSSG from total glutathione [27]. The GSH and GSSG Assay Kit was purchased from Beyotime Institute of Biotechnology (Nanjing, China).

#### Transmission electron microscopy (TEM)

The ultrastructure of *C. vulgaris*, treated and untreated with ZnO NPs, was observed by TEM (H-7650; Hitachi, Japan). After exposure for 72 h, *C. vulgaris*, treated or untreated with 20  $\mu\text{mol L}^{-1}$  ZnO NPs, was collected by centrifugation, followed by double fixation, dehydration, infiltration, embedding, and ultrathin sectioning for TEM analysis.

#### Statistical analysis

Experimental data were analyzed by use of the Origin 7.5 and SPSS 17.0 software packages in accordance with the methods provided by the manufacturers of the test kits. Each of the toxicity data sets was compared with its corresponding control. The differences were considered statistically significant when  $p$  was less than 0.05.

## Results and discussion

### Toxicity of ZnO NPs, $\text{Zn}^{2+}$ , and DCPD to *C. vulgaris*

The concentration–response curves obtained after treatment of *C. vulgaris* with ZnO NPs,  $\text{ZnSO}_4 \cdot 7\text{H}_2\text{O}$ , (*S*)-DCPD, and (*R*)-DCPD, and the ultrastructure of *C. vulgaris* treated and untreated with ZnO NPs are shown in Figs. S2–S4 (Electronic Supplementary Material). The TEM images show that ZnO NPs are toxic to *C. vulgaris* as a result of induction of ultrastructural alterations of the algal cells. ZnO NPs can be adsorbed by cells' membranes and a small amount of the NPs can enter the cells. This causes damage to chloroplasts and membranes in algal cells. The toxicity of all the materials tested was dose-dependent. Inhibition of algae by  $\text{ZnSO}_4 \cdot 7\text{H}_2\text{O}$ , used as a source of free zinc ions, was greater than that by the same concentration of ZnO NPs. This suggests that  $\text{Zn}^{2+}$  is more toxic than ZnO NPs. Inhibition of *C. vulgaris* by 50  $\mu\text{mol L}^{-1}$  (*S*)-DCPD and (*R*)-DCPD was 3.61 % and 8.52 %, respectively, after exposure for 72 h. Inhibition by (*R*)-DCPD seemed slightly greater than that by (*S*)-DCPD, which is consistent with the report by Wen et al. [28] that the (*R*) enantiomer induced greater production of ROS [28]. The toxicity of 50  $\mu\text{mol L}^{-1}$  DCPD to *C. vulgaris* was low compared with the toxicity of ZnO NPs and  $\text{ZnSO}_4 \cdot 7\text{H}_2\text{O}$ .

The toxicity to the algae of ZnO NPs at three concentrations combined with 50  $\mu\text{mol L}^{-1}$  DCPD is shown in Fig. 1a. Inhibition increased when *C. vulgaris* was exposed to ZnO NPs with DCPD, especially (*R*)-DCPD. The observed combined toxic effect correlated well with ZnO NPs concentration. The results indicated that DCPD enantioselectively increases the toxicity of nano-ZnO, and the combined toxicity was mainly attributed to ZnO concentration. Similar tendencies were also observed after treatment of *C. vulgaris* with

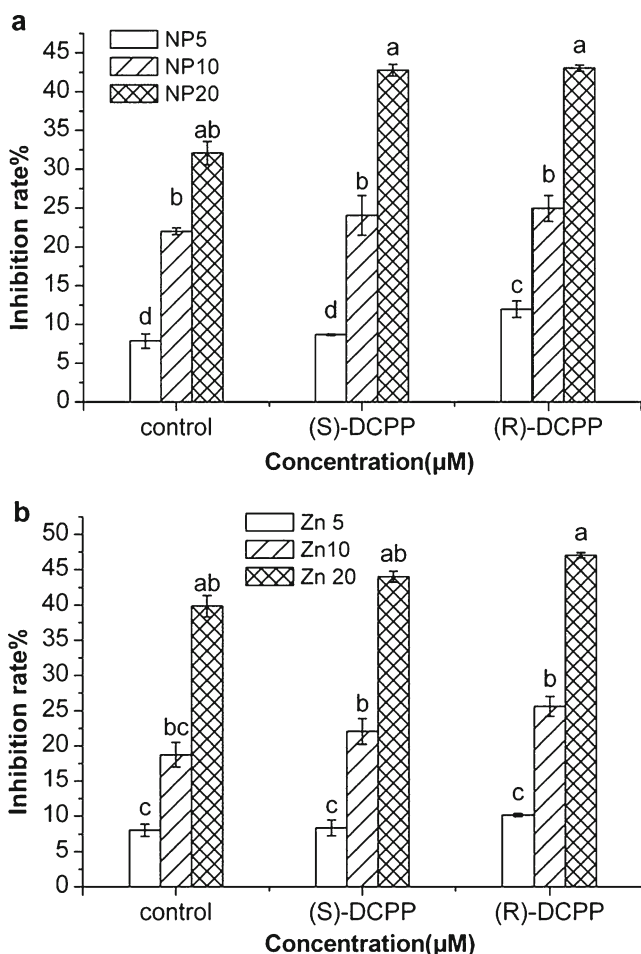


**Fig. 1** (a) Toxicity to *C. vulgaris* of ZnO NPs, with or without 50  $\mu\text{mol L}^{-1}$  DCPP, after 72 h. NP5, NP10, and NP20 indicate ZnO NP concentrations of 5  $\mu\text{mol L}^{-1}$ , 10  $\mu\text{mol L}^{-1}$ , and 20  $\mu\text{mol L}^{-1}$ , respectively. (b) Toxicity to *C. vulgaris* of  $\text{ZnSO}_4 \cdot 7\text{H}_2\text{O}$ , with or without 50  $\mu\text{mol L}^{-1}$  DCPP, after 72 h. Zn5, Zn10, and Zn20 indicate  $\text{ZnSO}_4 \cdot 7\text{H}_2\text{O}$  concentrations of 5  $\mu\text{mol L}^{-1}$ , 10  $\mu\text{mol L}^{-1}$ , and 20  $\mu\text{mol L}^{-1}$ , respectively. Bars with the same letter are not statistically significantly different ( $p < 0.05$ )

$\text{ZnSO}_4 \cdot 7\text{H}_2\text{O}$  and 50  $\mu\text{mol L}^{-1}$  DCPP (Fig. 1b). We therefore chose a concentration of 50  $\mu\text{mol L}^{-1}$  DCPP for subsequent research.

#### Release of Zinc Ion

The  $\text{Zn}^{2+}$  released from nano-ZnO, including intracellular zinc and zinc bound to the cell wall of *C. vulgaris*, were detected by ICP-MS. As shown in Fig. 2, the concentrations of both intracellular and cell-wall-bound zinc increased as the concentration of ZnO NPs increased. When *C. vulgaris* was treated with ZnO NPs (5  $\mu\text{mol L}^{-1}$ , 10  $\mu\text{mol L}^{-1}$ , and 20  $\mu\text{mol L}^{-1}$ ), the cell-wall-bound and intracellular  $\text{Zn}^{2+}$  concentrations were in the range 31.3–217.4  $\mu\text{g L}^{-1}$  and 4.11–14.6  $\mu\text{g L}^{-1}$ , respectively. Hence, most of the dissolved  $\text{Zn}^{2+}$  was bound to the cell walls of the algae. Similar results were reported by Ma et al. [29] and Wang et al. [26].

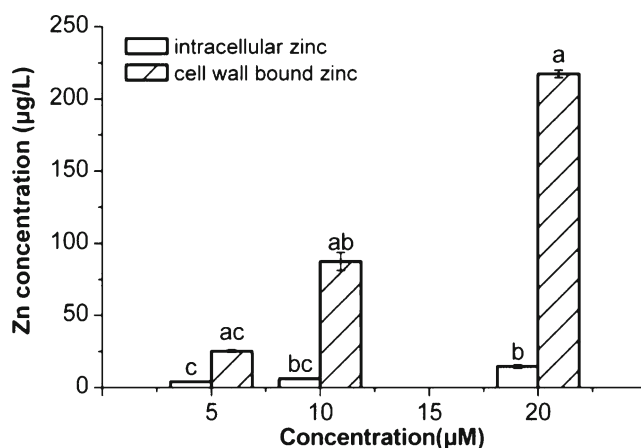


**Fig. 2** Contents of zinc dissolved in the intracellular of cells and bound to the cell wall of *C. vulgaris* exposed to different concentrations of ZnO NPs for 72 h. Bars with the same letter are not statistically significantly different ( $p < 0.05$ )

The cell wall is the first and primary barrier to uptake of NPs, and it has been reported that most of the algal cell wall consists of carbohydrates, including uronic acids [30], so most of the  $\text{Zn}^{2+}$  may combine with functional groups present in the algal cell wall. The amount of cell-wall-bound zinc was almost the same when algae were exposed to the same concentration of ZnO NPs and  $\text{ZnSO}_4 \cdot 7\text{H}_2\text{O}$  (Fig. 3a), but the concentration of intracellular zinc was significantly different ( $p < 0.05$ ) after these treatments (Fig. 3b). Free  $\text{Zn}^{2+}$  in culture medium after treatment with  $\text{ZnSO}_4 \cdot 7\text{H}_2\text{O}$  was greater than after treatment with the same concentration of ZnO NPs, because ZnO NPs did not dissolve completely. Inhibition of *C. vulgaris* by  $\text{ZnSO}_4 \cdot 7\text{H}_2\text{O}$  was greater than by ZnO NPs (Fig. S1). These results indicate that released  $\text{Zn}^{2+}$  was one of the causes of the toxicity of ZnO NPs and that the amount of intracellular zinc was important in the mechanism of toxicity.

#### Response of antioxidant defenses

Lipid peroxidation by *C. vulgaris* exposed to different concentrations of ZnO NPs was measured (Fig. 4). Lipid peroxidation is an indicator of oxidative damage to cell membrane lipids and has been used extensively as a biomarker of oxidative stress in vivo [31]. It is estimated by measuring the MDA content of cells. Increasing MDA values indicated that nano-ZnO caused dose-dependent oxidative damage. SOD activity varied with the concentration of nano-ZnO to which *C. vulgaris* was exposed. The highest SOD activity was observed after exposure to 5  $\mu\text{mol L}^{-1}$  nano-ZnO. SOD activity then decreased to 1.2, 1.1 times that of the control, with increasing nano-ZnO concentration. A similar phenomenon was reported by Hao et al. for different organs of carp; the activity of antioxidant enzymes followed a changing trend of being activated by low concentrations of nano-ZnO and inhibited by higher concentrations [13]. The activity of antioxidative

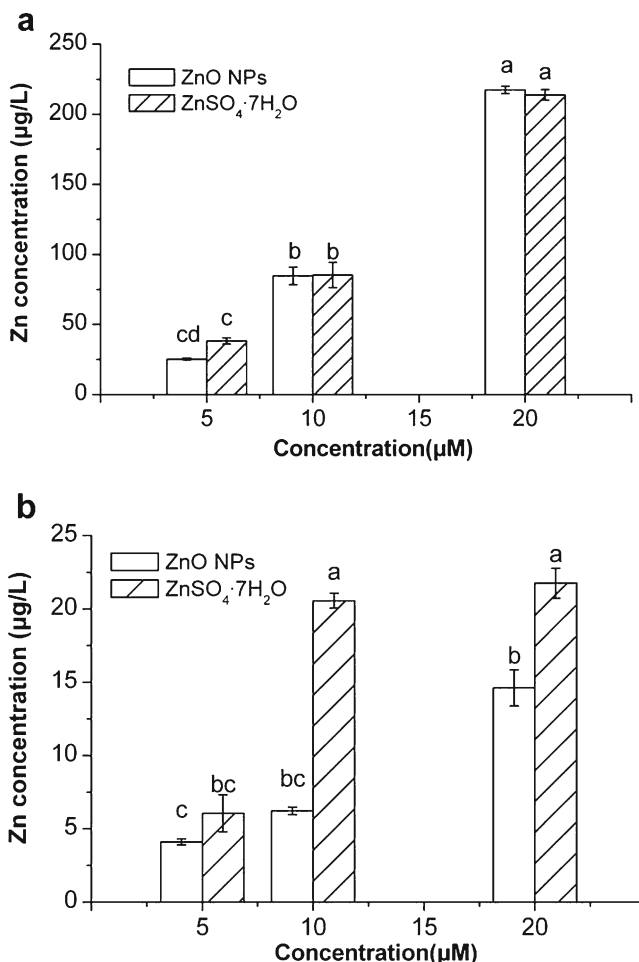


**Fig. 3** Concentrations of Zn<sup>2+</sup> bound to the cell wall (a) and in the intracellular contents (b) of *C. vulgaris* cells exposed to ZnO NPs and ZnSO<sub>4</sub>·7H<sub>2</sub>O (5 µmol L<sup>-1</sup>, 10 µmol L<sup>-1</sup>, and 20 µmol L<sup>-1</sup>). Bars with the same letter are not statistically significantly different (*p*<0.05)

enzymes in cells is in dynamic balance. For relatively low levels of exposure (5 µmol L<sup>-1</sup>), SOD activity was activated for self-protection. When the self-scavenging capacity of the antioxidant defense systems was exceeded by over-accumulation of free radicals caused by high nano-ZnO concentration, the activity of SOD decreased. These results

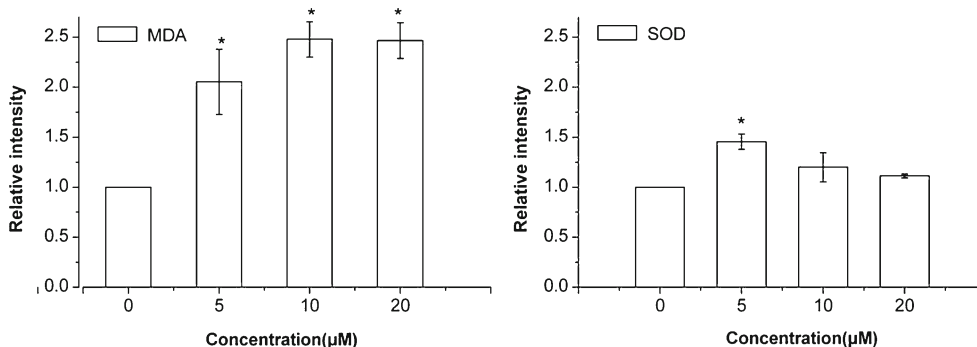


**Fig. 4** Relative expression of MDA and SOD in *C. vulgaris* after exposure to 0 µmol L<sup>-1</sup>, 5 µmol L<sup>-1</sup>, 10 µmol L<sup>-1</sup>, and 20 µmol L<sup>-1</sup> ZnO NPs for 72 h. MDA value and SOD activity for the control were normalized to 1 unit and values after other treatments were expressed relative to this value. Asterisks denote significant differences from the control at the 95 % confidence level

suggested that nano-ZnO could cause oxidative stress. However, the exact cause of this oxidative stress is difficult to determine, because ZnO NPs can also release Zn<sup>2+</sup> (Fig. 2) which can also cause this effect. Thus further experiments were conducted to determine the primary cause of oxidative stress.

#### Chiral perturbation of the glutathione redox cycle of *C. vulgaris*

The chiral perturbation approach introduced by Chen et al. [23] was used to assess whether the oxidative stress caused by NPs is responsible for the toxicity of ZnO NPs. The chiral chemical chosen as the chiral perturbation factor in the chiral perturbation approach should be enantioselective during the production of ROS and in the response of glutathione system. Its toxicity should also be too low to disturb the toxicity of ZnO NPs to *C. vulgaris*. The toxicity of ZnO NPs may result from direct induction of generation of ROS by the NPs and/or from zinc dissolved from the NPs. When *C. vulgaris* was exposed to the chiral chemical with ZnO NPs, an enantioselective shift in the glutathione system should be observed if induced generation of ROS is the cause of the toxicity of nano-ZnO. However, the chiral perturbation should be small enough not to induce enantioselective shift in the glutathione system when the dissolved zinc is mainly combined with GSH. In this research, the toxicity of the two enantiomers of DCPD was low enough compared with that of ZnO NPs and ZnSO<sub>4</sub>·7H<sub>2</sub>O. Compared with the control, an obvious decrease in GSH level and GSH/GSSG ratio was observed for algal cells treated with (*R*)-DCPD. However, an obvious difference in GSH level was not observed after treatment with (*S*)-DCPD, as shown in Fig. 5. (*R*)-DCPD, which induced production of ROS, caused the enantioselective response of the glutathione redox cycle to protect against algal cell damage. These results confirmed that DCPD was suitable to be chosen as the chiral perturbation factor.

(*R*)-DCPD and (*S*)-DCPD were added into the algae culture medium, with nano-ZnO or ZnSO<sub>4</sub>·7H<sub>2</sub>O, to assess the

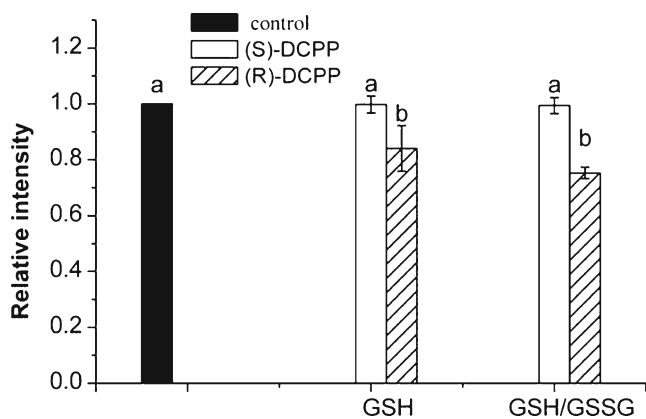


**Fig. 5** Effect of  $50 \mu\text{mol L}^{-1}$  of the two enantiomers of DCPP on the GSH cycle. GSH and GSH/GSSG levels for the control, were normalized to 1 and values after other treatments were expressed relative to this value. Bars with the same letter are not statistically significantly different ( $p < 0.05$ )

enantioselective shift in the glutathione system. When treatment was with nano-ZnO only, the changes in GSH level and GSH/GSSG ratio were small compared with the control. When treatment was with nano-ZnO and (R)-DCPP, there was an obvious decrease both in GSH level and in GSH/GSSG ratio, but this phenomenon was not observed after treatment with nano-ZnO and (S)-DCPP (Fig. 6). This revealed that ZnO NPs caused cell toxicity to *C. vulgaris* by aggravating the generation of ROS which resulted in the response of the glutathione system. Because free zinc ions can enhance production of ROS, further experiments were conducted with  $\text{ZnSO}_4 \cdot 7\text{H}_2\text{O}$  and DCPP to avoid the effect of dissolved  $\text{Zn}^{2+}$  on the glutathione system. As shown in Fig. 7, enantioselective differences were not observed when the algae were exposed to  $\text{ZnSO}_4 \cdot 7\text{H}_2\text{O}$  and the two enantiomers of DCPP. Also, after exposure to  $\text{ZnSO}_4 \cdot 7\text{H}_2\text{O}$ , levels of GSH and GSH/GSSG ratio decreased significantly compared

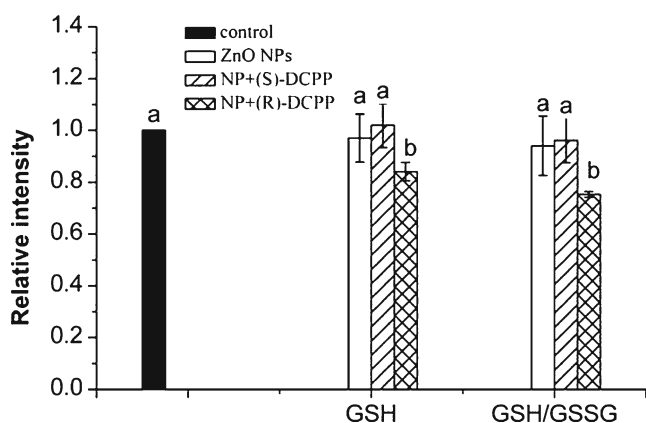


**Fig. 6** Change of GSH level and GSH/GSSG ratio in algal cells after exposure to  $20 \mu\text{mol L}^{-1}$  ZnO NPs, and  $20 \mu\text{mol L}^{-1}$  ZnO NPs with  $50 \mu\text{mol L}^{-1}$  (S)-DCPP or (R)-DCPP. GSH and GSH/GSSG levels for the control were normalized to 1 and values after other treatments were expressed relative to this value. Bars with the same letter are not statistically significantly different ( $p < 0.05$ )

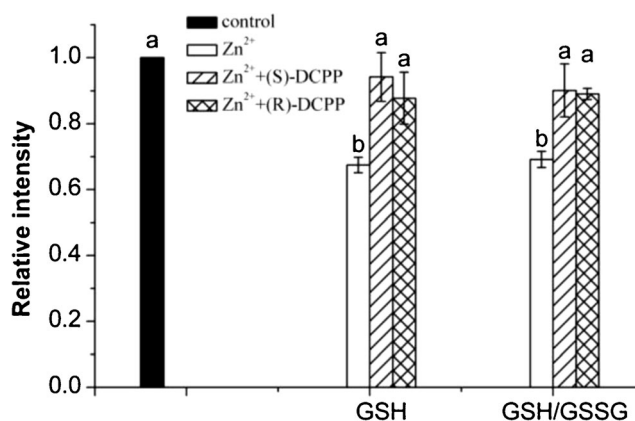


**Fig. 7** Change of GSH level and GSH/GSSG ratio in algal cells after exposure to  $20 \mu\text{mol L}^{-1}$   $\text{ZnSO}_4$ , and  $20 \mu\text{mol L}^{-1}$   $\text{ZnSO}_4$  with  $50 \mu\text{mol L}^{-1}$  (S)-DCPP or (R)-DCPP. GSH and GSH/GSSG levels for the control were normalized to 1 and values after other treatments were expressed relative to this value. Bars with the same letter are not statistically significantly different ( $p < 0.05$ )

with the control. The results demonstrated that  $\text{Zn}^{2+}$  ions were mainly bound to GSH in the glutathione system. Compared with  $\text{ZnSO}_4 \cdot 7\text{H}_2\text{O}$  treatment alone, the combined effect of DCPP and  $\text{ZnSO}_4 \cdot 7\text{H}_2\text{O}$  induced a rise in GSH production. Because the carboxyl group of DCPP can complex with metal ions to form complexes [28], there would be fewer free zinc ions to form GSH-Zn. All these results provided indirect evidence that the NP properties of ZnO NPs are the cause of the ROS which induce cell damage in *C. vulgaris*.

## Conclusions

On the basis of these experimental results we concluded that ZnO NPs were toxic to algae and the toxicity was dose-dependent. Analysis of  $\text{Zn}^{2+}$  concentrations indicated that although most of the zinc was bound to the cell wall, intracellular zinc is important in the toxicity of nano-ZnO. By assessment oxidative damage we demonstrated that ZnO NPs can cause oxidative stress. Enantioselectivity was clearly observed for GSH level and GSH/GSSG ratio after exposure to ZnO and DCPP together. Compared with treatment with  $\text{ZnSO}_4 \cdot 7\text{H}_2\text{O}$  and DCPP, however, the enantioselective shift in the dynamic glutathione system was not obvious. The chiral perturbation approach revealed that NPs could increase ROS production. In conclusion, the toxicity of ZnO NPs was caused by the properties of both the NPs and the zinc. Hence, the effect of neither the characteristics of the NPs themselves nor release of  $\text{Zn}^{2+}$  ion from the NPs should be ignored when evaluating the toxicity of ZnO NPs. To understand and mitigate the negative effects of these particles, methods and techniques should be further developed to thoroughly explain the mechanism(s) of the toxicity of nano-ZnO in future studies.

**Acknowledgements** The authors are very grateful to the Project of Science and Technology Department of Zhejiang Province (2012C37058) and the Key Innovation Team of Science and Technology in Zhejiang Province (2010R50018) for financial support.

## References

- Gottschalk F, Nowack B (2011) The release of engineered nanomaterials to the environment. *J Environ Monit* 13:1145–1155
- Pikethly MJ (2004) Nanomaterials—the driving force. *Materialstoday* 7:20–29
- Danovaro R, Bongiorno L, Corinaldesi C, Giovannelli D, Damiani E, Astolfi P, Greci L, Pusceddu A (2008) Sunscreens cause coral bleaching by promoting viral infections. *Environ Health Perspect* 116:441–447
- Wong SWY, Leung PTY, Djurišić AB, Leung KMY (2010) Toxicities of nano zinc oxide to five marine organisms: influences of aggregate size and ion solubility. *Anal Bioanal Chem* 396:609–618
- Franklin NM, Rogers NJ, Apte SC, Batley GE, Gadd GE, Casey PS (2007) Comparative toxicity of nanoparticulate ZnO, bulk ZnO, and ZnCl<sub>2</sub> to a freshwater microalga (*Pseudokirchneriella subcapitata*): the importance of particle solubility. *Environ Sci Technol* 41:8484–8490
- Aruoja V, Dubourguier H-C, Kasemets K, Kahru A (2009) Toxicity of nanoparticles of CuO, ZnO and TiO<sub>2</sub> to microalgae *Pseudokirchneriella subcapitata*. *Sci Total Environ* 407:1461–1468
- Ji J, Long Z, Lin D (2011) Toxicity of oxide nanoparticles to the green algae *Chlorella* sp. *Chem Eng J* 170:525–530
- Mingsheng X, Li J, Hanagata N, Huanxing S, Chen H, Fujita D (2013) Challenge to assess the toxic contribution of metal cation released from nanomaterials for nanotoxicology—the case of ZnO nanoparticles. *Nanoscale* 5:4763–4769
- Blinova I, Ivask A, Heinlaan M, Mortimer M, Kahru A (2009) Ecotoxicity of nanoparticles of CuO and ZnO in natural water. *Environ Pollut* 158:41–47
- Wiench K, Wohlleben W, Hisgen V, Radke K, Salinas E, Zok S, Landsiedel R (2009) Acute and chronic effects of nano- and non-nano-scale TiO<sub>2</sub> and ZnO particles on mobility and reproduction of the freshwater invertebrate *Daphnia magna*. *Chemosphere* 76:1356–1365
- Li M, Lin D, Zhu L (2013) Effects of water chemistry on the dissolution of ZnO nanoparticles and their toxicity to *Escherichia coli*. *Environ Pollut* 173:97–102
- Zhu X, Zhu L, Duan Z, Qi R, Li Y, Lang Y (2008) Comparative toxicity of several metal oxide nanoparticle aqueous suspensions to Zebrafish (*Danio rerio*) early developmental stage. *J Environ Sci Health A* 43:278–284
- Hao L, Chen L (2012) Oxidative stress responses in different organs of carp (*Cyprinus carpio*) with exposure to ZnO nanoparticles. *Ecotoxicol Environ Saf* 80:103–110
- Sharifi S, Behzadi S, Laurent S, Laird Forrest M, Stroeve P, Mahmoudi M (2012) Toxicity of nanomaterials. *Chem Soc Rev* 41:2323–2343
- Pisanic TR, Jin S, Shubayev VI (2009) *Nanotoxicity: From in vivo and In vitro models to health risks*. John Wiley & Sons, Ltd., London, UK, pp 397–425
- De Berardis B, Civitelli G, Condello M, Lista P, Pozzi R, Arancia G, Meschini S (2010) Exposure to ZnO nanoparticles induces oxidative stress and cytotoxicity in human colon carcinoma cells. *Toxicol Appl Pharmacol* 246:116–127
- Ma H, Williams PL, Stephen A (2013) Diamond Ecotoxicity of manufactured ZnO nanoparticles—A review. *Environ Pollut* 172:76–85
- Lu J, Zhang S, Luo L, Han W, Zhang J, Yang K, Christie P (2012) Dissolution and Microstructural Transformation of ZnO Nanoparticles under the Influence of Phosphate. *Environ Sci Technol* 46:7215–7221
- Li M, Zhu L, Lin D (2012) Toxicity of ZnO Nanoparticles to *Escherichia coli*: Mechanism and the Influence of Medium Components. *Environ Sci Technol* 45:1977–1983
- Maynard AD, Aitken RJ, Butz T, Colvin V, Donaldson K, Oberdorster G, Philbert MA, Ryan J, Seaton A, Stone V, Tinkle SS, Tran L, Walker NJ, Warheit DB (2006) Safe handling of nanotechnology. *Nature* 444:267–269
- Foyer CH, Noctor G (2011) Ascorbate and glutathione: the heart of the redox hub. *Plant Physiol* 155:2–18
- Sies H (1999) Glutathione and its role in cellular functions. *Free Radic Biol Med* 27:916–921
- Chen H, Chen J, Guo Y, Wen Y, Liu J, Liu W (2012) Evaluation of the role of the glutathione redox cycle in Cu(II) toxicity to green algae by a chiral perturbation approach. *Aquat Toxicol* 120–121:19–26
- Garrison AW (2006) Probing the enantioselectivity of chiral pesticides. *Environ Sci Technol* 40:16–23
- Wen YZ, Li CD, Fang ZH, Zhuang SL, Liu WP (2011) Elucidation of the enantioselective enzymatic hydrolysis of chiral herbicide dichlorprop methyl by chemical modification. *J Agric Food Chem* 59:1924–1930
- Wang Z, Li J, Zhao J, Xing B (2011) Toxicity and Internalization of CuO Nanoparticles to Prokaryotic Alga *Microcystis aeruginosa* Affected by Dissolved Organic Matter. *Environ Sci Technol* 45:6032–6040
- Rahman I, Kode A, Biswas SK (2006) Assay for quantitative determination of glutathione and glutathione disulfide levels using enzymatic recycling method. *Nat Protoc* 1:3159–3164
- Wen Y, Chen H, Shen C, Zhao M, Liu W (2011) Enantioselectivity Tuning of Chiral Herbicide Dichlorprop by Copper: Roles of Reactive Oxygen Species. *Environ Sci Technol* 45:4778–4784
- Ma M, Zhu W, Wang Z, Witkamp GJ (2003) Accumulation, assimilation and growth inhibition of copper on freshwater alga (*Scenedesmus subspicatus* 86.81 SAG) in the presence of EDTA and fulvic acid. *Aquat Toxicol* 63:221–228
- Blumerisinger M, Meindl D, Loos E (1983) Cell wall composition of chlorococcal algae. *Phytochemistry* 22:1603–1604
- Sayeed I, Parvez S, Pandey S, Bin-Hafeez B, Haque R, Raisuddin S (2003) Oxidative stress biomarkers of exposure to deltamethrin in freshwater fish, *Channa punctatus* Bloch. *Ecotoxicol Environ Saf* 56:295–301